DOI: 10.1002/asia.200600230

Energy Landscape of Aptamer/Protein Complexes Studied by Single-Molecule Force Spectroscopy

Junping Yu,[a] Yaxin Jiang,[a, b] Xinyong Ma,[a] Yi Lin,[a] and Xiaohong Fang*[a]

Abstract: Aptamers are single-stranded nucleic acid molecules selected in vitro to bind to a variety of target molecules. Aptamers bound to proteins are emerging as a new class of molecules that rival commonly used antibodies in both therapeutic and diagnostic applications. With the increasing application of aptamers as molecular probes for protein recognition, it is important to understand the molecular mechanism of aptamer–protein interaction. Recently, we developed a method of using atomic force microscopy (AFM) to study the single-molecule rupture force of aptamer/protein complexes. In this work, we investigate further the unbinding dynamics of aptamer/protein complexes and their dissociation-energy landscape by AFM. The dependence of single-molecule force on the AFM loading rate was plotted for three aptamer/protein complexes and their dissociation rate constants, and other parameters characterizing their dissociation pathways were obtained. Furthermore, the single-molecule force spectra of three aptamer/protein complexes were compared to those of the corresponding antibody/protein complexes in the same loading-rate range. The results revealed two activation barriers and one intermediate state in the unbinding process of aptamer/protein complexes, which is different from the energy landscape of antibody/protein complexes. The results provide new information for the study of aptamer–protein interaction at the molecular level.

Keywords: aptamers · atomic force microscopy · energy landscape · proteins

Introduction

Aptamers are 20–60-nt single-stranded DNA or RNA molecules isolated from synthetic nucleic acid libraries by in vitro selection processes to bind to a variety of targets ranging from metal ions, amino acids, peptides, and proteins to cells and tissues.[1,2] The development and application of aptamers that specifically recognize protein targets and modulate their biological functions through binding with their functional domains have attracted particular attention.[3,4] In comparison with commonly used antibodies, aptamers have many advantages, including simpler synthesis, easier storage, faster tissue penetration, easier modification, and wider applicability. They are emerging as a new class of protein probes that rival antibodies in both diagnostic and therapeutic applications. For a better understanding of how aptamers interact with their protein targets, several methods, such as NMR and fluorescence spectroscopy and X-ray diffraction, have been used to study the binding mechanism and properties of aptamer/protein complexes.[4,5]

Recently, we developed a new method of studying the interaction between protein and aptamer by AFM at the single-molecule level.[6,7] AFM has the capability to measure the force governing biomolecular recognition under physiological conditions with piconewton (pN) sensitivity.[8–11] The single-molecule rupture force of immunoglobulin E (IgE) and its 37-nt DNA aptamer has been obtained and compared with that of IgE and its monoclonal antibody.[6,12] The results revealed the high affinity of the aptamer toward the protein, which could match or even surpass that of the antibody to the antigen.

Besides the measurement of rupture forces for noncovalent ligand–receptor bonds, AFM is also advantageous in offering information on the prominent barriers traversed in the energy landscape along their force-drive unbinding pathways.[13–18] Single-molecule dynamic force spectroscopy has provided new insight into the complexity of macromolecular noncovalent interaction. It has been applied to exploring the

[a] J. Yu,[+] Dr. Y. Jiang,[+] X. Ma, Y. Lin, Prof. X. Fang
Beijing National Laboratory for Molecular Sciences
Institute of Chemistry, Chinese Academy of Sciences
Beijing 100080 (China)
Fax: (+86) 10-62650024
E-mail: xfang@iccas.ac.cn

[b] Dr. Y. Jiang[+]
Institute of Physics, Chinese Academy of Sciences
Beijing 100080 (China)

[+] Equal contribution from the first two authors.

WILEY InterScience DISCOVER SOMETHING GREAT

© 2007 Wiley-VCH Verlag GmbH & Co. KGaA, Weinheim

energy landscape of intermolecular bonds for small-molecule ligand/protein,[13–16] antibody/antigen,[17] and other ligand/receptor pairs.[18] Herein, we report the first attempt at studying the energy landscape of aptamer/protein complexes. The rupture forces of three aptamer/protein complexes (two IgE aptamer/IgE complexes and one thrombin aptamer/thrombin complex) were measured under different AFM loading rates. The dynamic force spectra of the aptamer/protein complexes were compared with those of the antibody/protein complexes. The results show that the unbinding of the aptamer/protein complex undergoes multiple transition states and overcomes two activation barriers before final separation. On the contrary, the unbinding of the antibody/protein complex has only one activation barrier in the same loading-rate range. The results provide new information for the understanding of the protein-binding nature of aptamers.

Abstract in Chinese:

核酸适体是指通过体外筛选得到的能特异结合不同靶分子的单链核酸分子。能与蛋白质特异结合的核酸适体在医学治疗和诊断领域的应用可与抗体相媲美。由于核酸适体被日益广泛地用于蛋白质的分子识别，深入了解核酸适体与蛋白质相互作用的分子机理非常重要。最近，我们发展了原子力显微镜 (AFM) 单分子力谱法研究核酸适体与蛋白质复合物的单分子解离力。在本论文的工作中，我们进一步利用 AFM 研究了核酸适体/蛋白质的解离动力学过程及解离能垒，得到了三对核酸适体/蛋白质复合物单分子解离力随 AFM 加载速率变化的曲线，并得到了它们的解离速率常数和其它与解离途径相关的参数。此外，我们还在同样的加载速率范围内将三对核酸适体/蛋白质的单分子力谱与相应的抗体/蛋白质进行了比较。结果表明与抗体/蛋白质的解离途径不同，核酸适体/蛋白质的解离要经过一个中间态，克服两个活化能垒。这些结果为在分子水平研究核酸适体和蛋白质之间的相互作用提供了新的信息。

Results and Discussion

Direct Single-molecular Force Measurement of IgE with Its Two Aptamers

First, we carried out direct measurement of single-molecule rupture force of the aptamer/IgE complex. The experiment was performed with IgE-modified AFM tips and DNA aptamer modified silicon substrates (Figure 1).[6,7] The protein was coupled to the AFM tip through a 20–40-nm long poly(ethylene glycol) (PEG) cross-linker to differentiate specific from nonspecific force.[19–21] The low density of the immobilized protein was used to ensure that only one aptamer/protein pair formed in the contact area of the tip and substrate. Thus, rupture forces from single aptamer/protein pairs were obtained. As shown in the typical force–distance curves in Figure 2a, the randomly appearing first peaks were caused by the nonspecific force between the tip and substrate, whereas the second peaks, which appeared about 20–40 nm away from the separation of the tip and substrate, represent the specific force between the protein and aptamer.[8,21] After injection of the solution of free protein ([IgE] = 5 μg mL^{-1}) or free aptamer (1×10^{-7} mol L^{-1}) into the AFM liquid cell, the first peaks did not change much, but the second peaks disappeared (Figure 2b). This confirmed that the second peaks were caused by the specific interaction of the aptamer and protein; thus, they were counted for further analysis.

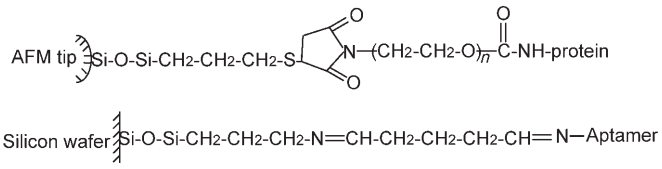

Figure 1. Schematic structures of the samples immobilized on the AFM tip and substrate.

The statistical distribution of the force values for IgE and its 37-nt aptamer, AP1, is plotted in Figure 2c. The single-molecular rupture force of AP1/IgE was determined to be (104 ± 0.6) pN at a loading rate of 1.9×10^5 pN s^{-1}. The average rupture force of AP1/IgE from three independent experiments was (103.8 ± 2.5) pN. This value is lower than what we reported before ((160 ± 29) pN at a similar loading rate).[6] In the previous work, the single-molecule force was derived indirectly by Poisson statistical methods from the measurement of the total forces of several pairs of aptamer/protein molecules. Besides the difference in experimental method, the uncalibrated spring constants of the tips used in the previous work may also contribute to the difference in the value of the single-molecule force.

We also measured the force between IgE and another 29-nt IgE aptamer, AP2, which has a shorter sequence. The dissociation constant of AP2/IgE (K_d = 82 nM) is higher than that of AP1/IgE (K_d = 10 nM).[12] Figure 2d displays the force histogram obtained by the same IgE-modified AFM tip and AP2-modified substrate. Although the binding probability of AP2/IgE was about the same as that of AP1/IgE (≈20%), the single-molecule rupture force of AP2/IgE was lower (peak value at (98.9 ± 0.9) pN in Figure 2d, average single-molecule force was (96.5 ± 2.1) pN at 1.9×10^5 pN s^{-1}). With a higher dissociation constant, AP2 should have a weaker binding capability with IgE. As the single-molecule forces of AP1/IgE and AP2/IgE were measured under the same experimental conditions except for the different aptamer-modified substrates, the results show a lower rupture force for the weaker binding of the aptamer/IgE complex.

Dependence of Single-Molecule Force between IgE and Aptamer on Loading Rate

It is known that for a noncovalent bond, its strength and lifetime measured by AFM are dynamic properties. They are dependent on the force loading rate, which is deter-

 © 2007 Wiley-VCH Verlag GmbH & Co. KGaA, Weinheim

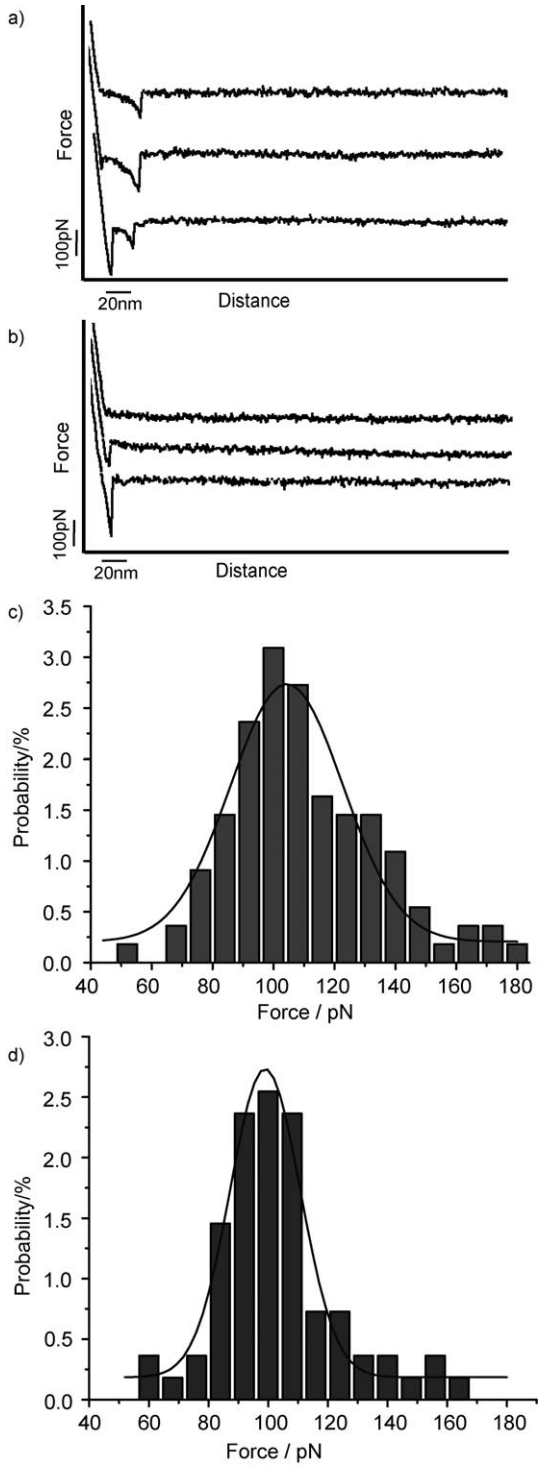

Figure 2. a) and b) Typical force–distance curves with IgE-modified AFM tip and AP1-modified substrates (a) and after a solution of free IgE was injected into the fluid cell to block the specific binding of AP1/IgE (b). c) and d) Histograms of the single-molecule rupture forces of AP1/IgE (c) and AP2/IgE (d) at a loading rate 1.9×10^5 pN s^{-1}. ■ = experimental data, —— = Gaussian fit curve.

mined by the product of the cantilever force constant and tip retraction velocity applied during the rupturing of a bond.[22–25]

According to the Bell model,[26] if a force F is applied in the direction favoring the unbinding of the aptamer/protein complex, the activation energy for complex dissociation will decrease and the dissociation off-rate will increase according to Equations (1) and (2):

$$\Delta E^{\neq}(F) = \Delta E^{\neq} - \chi_\beta \cdot F \quad (1)$$

$$k_{off}(F) = k_{off}(0) \cdot e^{F \cdot x_\beta / k_B T} \quad (2)$$

where $\Delta E^{\neq}$ and $k_{off}(0)$ are the activation energy and off-rate constant of the aptamer/protein complex in the absence of force, and $\Delta E^{\neq}(F)$ and $k_{off}(F)$ are the corresponding variables in the presence of applied force. χ_β is the difference in separation of the ligand and receptor between the bound and transition states along the direction of the applied force, k_B is the Boltzmann constant, and T is the absolute temperature. Therefore, if the pulling force is assumed to increase at a constant rate r, the most-probable unbinding force F is given by [Eq. (3)]:[22–25]

$$F = \frac{k_B T}{\chi_\beta} \cdot \ln\left(\frac{r\chi_\beta}{k_{off}(0) k_B T}\right) = \frac{k_B T}{\chi_\beta} \cdot \ln r + \frac{k_B T}{\chi_\beta} \cdot \ln\left(\frac{\chi_\beta}{k_{off}(0) k_B T}\right) \quad (3)$$

Equation (3) predicts a linear relationship between the individual unbinding force F and $\ln r$. From the slope and the intercept in the plot of F versus $\ln r$, information on the dissociation of the complex (Bell model parameters), such as χ_β, k_{off}, and the binding lifetime τ ($=1/k_{off}$), can be derived.

We performed the dynamic force measurement for the aptamer/protein complex at different loading rates of 1.2×10^4–1.7×10^6 pN s^{-1}. At each loading rate, the single-molecule force was obtained by Gaussian fit of force histograms from three independent experiments. The dynamic force spectra of AP1/IgE and AP2/IgE are shown in Figure 3a. With increasing loading rate, the rupture force of the aptamer/protein complex displayed an initial gradual increase followed by a more-rapid increase at higher loading rates. The two distinct linear regions indicate that the dissociation of the aptamer/protein complex passed through at least two energy barriers and two transition states.[15] As shown in Table 1, the higher-force region (loading-rate range of 3.8×10^5–1.7×10^6 pN s^{-1}) defined the inner energy barriers at 0.91 Å for AP1/IgE and 1.09 Å for AP2/IgE. Their off-rate constants and bond-survival times extrapolated to zero force were 607 s^{-1} and 0.0016 s and 577 s^{-1} and 0.0017 s, respectively. The lower-force region (loading-rate range of 1.2×10^4–3.8×10^5 pN s^{-1}) mapped the outer energy barriers at 2.54 Å for AP1/IgE and 2.78 Å for AP2/IgE. Their off-rate constants and bond-survival times extrapolated to zero force were 16.36 s^{-1} and 0.061 s and 18.92 s^{-1} and 0.053 s, respectively.

According to transition-state theory, the dissociation rate constant is a function of the activation energy ΔE [Eq. (4)]:[13,15]

 © 2007 Wiley-VCH Verlag GmbH & Co. KGaA, Weinheim

CHEMISTRY
AN ASIAN JOURNAL

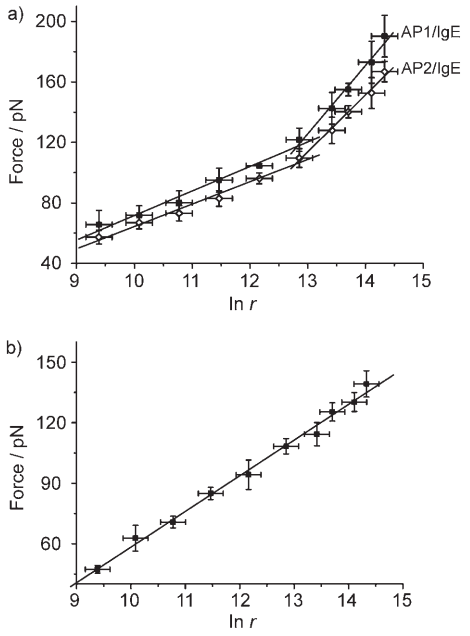

Figure 3. Most-probable individual rupture force (determined by a Gaussian fit of force distribution such as that in Figure 2c or d) of a) AP1/IgE and AP2/IgE and b) antibody/IgE at different loading rates. Data are shown as the mean and standard errors from three independent experiments.

Table 1. Bell model parameters from F versus $\ln r$.

Ligand/Receptor	Loading-rate range [pN s^{-1}]	χ_β [Å]	k_{off} [s^{-1}]	τ [s]	$\Delta\Delta E$[a] [k_BT]
AP1/IgE	1.2×10^4–3.8×10^5	2.54	16.36	0.061	
	3.8×10^5–1.7×10^6	0.91	607	0.0016	
AP2/IgE	1.2×10^4–3.8×10^5	2.78	18.92	0.053	−0.145
	3.8×10^5–1.7×10^6	1.09	577	0.0017	0.051
antibody/IgE	1.2×10^4–1.7×10^6	3.60	46.1	0.022	
aptamer/α-thrombin	1.2×10^4–2.0×10^5	3.20	2.06	0.49	
	2.0×10^5–1.7×10^6	0.67	517	0.0020	
antibody/α-thrombin	1.2×10^4–1.7×10^6	2.51	8.57	0.12	

[a] Relative to the AP1/IgE binding energy.

$$k_{off} \propto e^{\frac{-\Delta E}{k_B T}} \quad (4)$$

Therefore, the differences in activation energy ($\Delta\Delta E = \Delta E(\mathrm{AP2}) - \Delta E(\mathrm{AP1})$) of the two analogous systems, AP2/IgE and AP1/IgE, can be derived by Equations (5)and (6):

$$k_{off}(\mathrm{AP2})/k_{off}(\mathrm{AP1}) = e^{\frac{-\Delta\Delta E}{k_B T}} \quad (5)$$

$$\Delta\Delta E = -k_B T \cdot \ln(k_{off}(\mathrm{AP2})/k_{off}(\mathrm{AP1})) \quad (6)$$

Thus, we calculated that the difference in energy barrier between AP2/IgE and AP1/IgE is $0.051k_BT$ for the inner and $-0.145k_BT$ for the outer barrier. It is expected that the lowering of the outer activation-energy barrier contributed to the weaker IgE binding capability of AP2 relative to AP1.

Dependence of Single-Molecule Force between IgE and Its Antibody on Loading Rate

We were interested in probing the energy landscape of antibody/IgE unbinding with protein-modified tips and antibody-modified substrates under the same experimental conditions. At each loading rate, the measured single-molecule force of the antibody/IgE complex was smaller than that of AP1/IgE, thus confirming the weaker affinity of the antibody/IgE complex as we previously reported.[6] Moreover, there was a significant difference in the dependence of the single-molecule force on loading rate between the antibody/IgE and aptamer/IgE complexes. In the whole loading-rate range, there was only one linear region in the plot of F versus $\ln r$ (Figure 3b), which suggests the presence of one activation barrier at 3.60 Å along the reaction coordinate. The dissociation rate constant and bond lifetime at zero pulling force were calculated to be 46.1 s^{-1} and 0.022 s, respectively (Table 1). These results indicate that the unbinding process and dissociation behavior of the aptamer/protein and antibody/protein complexes were different in the loading-rate range studied.

Energy Landscapes of Aptamer/α-Thrombin and Antibody/α-Thrombin Complexes

To examine if other aptamer/protein complexes have the same characteristics in their energy landscapes, we studied the unbinding dynamics of another aptamer/protein pair, aptamer/α-thrombin, as well as antibody/α-thrombin in the same loading-rate range.[27] Figure 4 shows that the plot of

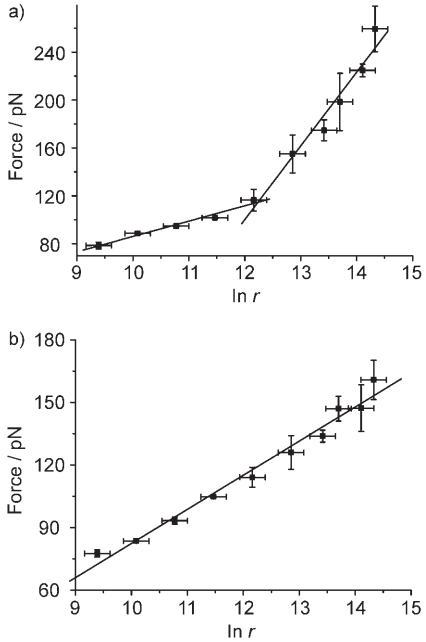

Figure 4. Most-probable individual rupture force of a) aptamer/α-thrombin and b) antibody/α-thrombin at different loading rates. Data are shown as the mean and standard errors from three independent experiments.

 © 2007 Wiley-VCH Verlag GmbH & Co. KGaA, Weinheim

single-molecular force of aptamer/α-thrombin versus $\ln r$ consists of two linear regions, but that of antibody/α-thrombin has only one. The Bell model parameters for both aptamer/α-thrombin and antibody/α-thrombin complexes are listed in Table 1. As with AP1/IgE and AP2/IgE, the unbinding of the aptamer/α-thrombin complex is not a simple process from the bound state to the dissociated state, but has one intermediate state and two activation barriers. However, the unbinding of the antibody/α-thrombin complex only passes through one activation barrier from the bound to the dissociated state.

In previous studies of the energy landscapes of protein complexes, it was found that the unbinding of protein with a small-molecule ligand, such as biotin/streptavidin and biotin/avidin, usually contains two activation barriers, whereas some antibody/antigen complexes have one.[13–18] On the basis of the results from our three aptamer/protein complexes, we suggest that the aptamer/protein complex may undergo the unbinding process with more than one activation barrier, similar to proteins with a small-molecule ligand. As the binding mechanism of the aptamer/protein complex is largely unknown, whether this is a general rule for aptamer/protein complexes, as well as the origin of the activation barriers, remain a question. However, our results demonstrate that in contrast to antibodies, the natural protein probes, man-made probe aptamers have different binding properties and dissociation pathways with their target proteins.

Conclusions

We have measured individual rupture forces of three aptamer/protein complexes, AP1/IgE, AP2/IgE, and aptamer/α-thrombin, under different loading rates. On the basis of the experimental results, we propose that the unbinding of aptamer/protein complexes is not a direct process, but has at least one intermediate state with two activation barriers to overcome. In contrast, the dynamic force spectra of the corresponding antibody/protein complexes obtained under the same loading-rate range as the aptamer/protein complexes showed only one activation barrier for the unbinding process. This indicates that although both aptamers and antibodies can bind to proteins with high affinity and specificity, the aptamer/protein complex undergoes a different dissociation process from the antibody/antigen complex.

Experimental Section

Materials

IgE, purified from human plasma, was purchased from Athens Research & Technology Inc. (Athens, GA, USA). Antihuman IgE (ε-chain specific), developed in goat-fractionated antiserum, was obtained from Sigma (St. Louis, MO, USA). Human α-thrombin and anti-thrombin antibody were purchased from Haematologic Technologies Inc. (Essex Junction, VT, USA). Amine-modified IgE aptamer 1 (AP1; 5′-NH_2-GGGGC ACGTT TATCC GTCCC TCCTA GTGGC GTGCCCC-3′), amine-modified IgE aptamer 2 (AP2; 5′-NH_2-CACGT TTATC CGTCC CTCCT AGTGG CGTG-3′), and amine-modified α-thrombin DNA aptamer (5′-NH_2-TTTTG GTTGG TGTGG TTGGTTT-3′) were all synthesized from SBS Genetech Co. Ltd. (Beijing, China). ω-*N*-hydroxysuccinimide ester–poly(ethylene glycol)–α-maleimide (MW 3400) (NHS-PEG-MAL) was obtained from Nektar Therapeutics (Huntsville, AL, USA). (3-Mercaptopropyl)trimethoxysilane (MPTMS), 3-aminopropyltriethoxysilane (APTES), and toluene (99.99%, HPLC grade) were obtained from ACRO (USA). Other reagents used in all experiments were of analytical grade. Milli-Q-purified water (18.2 MΩ) was used for all experiments.

Preparation and Modification of Silicon Substrates and AFM Tips

According to the previously reported procedures,[6] single-crystal silicon wafers were cut into 1.5 cm × 1.5 cm squares and cleaned. The cleaned wafers were transferred to a solution of APTES (1.0% *v*/*v*) in toluene and incubated for 2 h at room temperature. The unbound silanes were then washed away by extensive rinsing with toluene. The silanized wafers were activated by incubation in a solution of glutaraldehyde (0.1% *v*/*v*) in phosphate-buffered saline (PBS) buffer (10 mM Na_2HPO_4, 1.8 mM KH_2PO_4, 2.7 mM KCl, 140 mM NaCl, pH 7.4) for the IgE system or Tris/HCl buffer (20 mM Tris-HCl buffer with 140 mM NaCl, 5 mM KCl, 1 mM $CaCl_2$, 1 mM $MgCl_2$, pH 7.4) for the α-thrombin system for 0.5 h at room temperature and then rinsed with buffer. The activated wafers were immersed in the solution of aptamer (1.0×10^{-7} M in buffer) at 4 °C for 10 h or the solution of antibody (5 μg mL^{-1} in buffer) at 4 °C for 1 h to couple the aptamer or antibody to the substrates.

Silicon nitride AFM tips (type: NP, Veeco, Santa Barbara, CA, USA) were used in the experiments. The spring constants of the tips, calibrated by the thermal fluctuation method,[28] fell in the range 0.040–0.065 N m^{-1}. The tip-cleaning procedure was the same as that previously reported.[6] The cleaned tips were transferred to a solution of MPTMS (1.0% *v*/*v*) in toluene, incubated for 2 h at room temperature, and then rinsed thoroughly with toluene to remove any unbound silane. The silanized tips were activated by incubation in NHS-PEG-MAL (1 mg mL^{-1}) in dimethyl sulfoxide for 3 h at room temperature,[29] and then rinsed extensively with dimethyl sulfoxide to remove any unbound NHS-PEG-MAL. The activated tips were immersed in a solution of protein (5 μg mL^{-1} IgE in PBS buffer or 2 μg mL^{-1} α-thrombin in Tris/HCl buffer) and incubated at room temperature for 0.5 h. After they were rinsed with buffer, the functionalized tips were stored in the buffer at 4 °C until use.

AFM Force Spectroscopy Measurements

A Nano Scope IV atomic force microscope (Veeco, Santa Barbara, CA) was used to carry out force measurements in a liquid cell filled with freshly prepared buffer (PBS buffer for the IgE system and Tris/HCl buffer for the α-thrombin system). Force measurements were performed with protein-functionalized tips and aptamer- or antibody-modified silicon wafers. In the loading-rate-dependent force measurements, the loading rate (pN s^{-1}) was determined by multiplying the cantilever retraction rate (nm s^{-1}) with the cantilever spring constant (pN nm^{-1}), and loading rates ranging from 1.20×10^4 to 1.7×10^6 pN s^{-1} were achieved by changing the cantilever velocity.[8,18,21] The ramp delay was set to 500 ms. Force–distance curves were recorded and analyzed with the Nanoscope 5.30b4 software (Veeco, Santa Barbara, CA). For each measurement, about 200 force values were used to construct a force histogram. The most-probable single-molecular interaction force was determined by fitting a Gaussian distribution to the force histogram.

Acknowledgements

We thank Prof. Chunli Bai (Institute of Chemistry) for valuable help. This work was supported by the National Natural Science Foundation of China (Nos. 20225516, 30490174, 10334100) and the Chinese Academy of Sciences (kjcx2-sw-h12).

 © 2007 Wiley-VCH Verlag GmbH & Co. KGaA, Weinheim

[1] C. Tuerk, L. Gold, *Science* **1990**, *249*, 505–510.
[2] A. D. Ellington, J. W. Szostak, *Nature* **1990**, *346*, 818–822.
[3] J. Wang, Z. H. Cao, Y. X. Jiang, C. S. Zhou, X. H. Fang, W. H. Tan, *IUBMB Life* **2005**, *57*, 123–128.
[4] S. D. Jayasena, *Clin. Chem.* **1999**, *45*, 1628–1650.
[5] T. Hermann, D. J. Patel, *Science* **2000**, *287*, 820–825.
[6] Y. X. Jiang, C. F. Zhu, L. S. Ling, L. J. Wan, X. H. Fang, C. L. Bai, *Anal. Chem.* **2003**, *75*, 2112–2116.
[7] Y. X. Jiang, J. Wang, X. H. Fang, C. L. Bai, *J. Nanosci. Nanotechnol.* **2004**, *4*, 611–615.
[8] P. Hinterdorfer, W. Baumgartner, H. J. Gruber, K. Schilcher, H. Schindler, *Proc. Natl. Acad. Sci. USA* **1996**, *93*, 3477–3481.
[9] Y. X. Jiang, F. Qin, Y. Q. Li, X. H. Fang, C. L. Bai, *Nucleic Acids Res.* **2004**, *32*, e101.
[10] J. Zlatanova, S. M. Lindsay, S. H. Leuba, *Prog. Biophys. Mol. Biol.* **2001**, *74*, 37–61.
[11] D. P. Allison, P. Hinterdorfer, W. H. Han, *Curr. Opin. Biotechnol.* **2002**, *13*, 47–51.
[12] T. W. Wiegand, P. B. Williams, S. C. Dreskin, M. H. Jouvin, J. P. Kinet, D. Tasset, *J. Immunol.* **1996**, *157*, 231–238.
[13] E. Evans, *Faraday Discuss.* **1998**, *111*, 1–16.
[14] R. Merkel, P. Nassoy, A. Leung, K. Ritchie, E. Evans, *Nature* **1999**, *397*, 50–53.
[15] C. Yuan, A. Chen, P. Kolb, V. T. Moy, *Biochemistry* **2000**, *39*, 10219–10223.
[16] Y. S. Lo, Y. J. Zhu, T. P. Beebe, Jr., *Langmuir* **2001**, *17*, 3741–3748.
[17] F. Schwesinger, R. Ros, T. Strunz, D. Anselmett, H. J. Güntherodt, A. Honegger, L. Jermutus, L. Tiefenauer, A. Plückthun, *Proc. Natl. Acad. Sci. USA* **2000**, *97*, 9972–9977.
[18] Y. Bustanji, C. R. Arciola, M. Conti, E. Mandello, L. Montanaro, B. Samori, *Proc. Natl. Acad. Sci. USA* **2003**, *100*, 13292–13297.
[19] P. Hinterdorfer, F. Kienberger, A. Raab, H. J. Gruber, W. Baumgartner, G. Kada, C. Riener, S. Wielert-Badt, C. Borken, H. Schindler, *Single Mol.* **2000**, *1*, 99–103.
[20] F. Kienberger, V. P. Pastushenko, G. Kada, H. J. Gruber, C. Riener, H. Schindler, P. Hinterdorfer, *Single Mol.* **2000**, *1*, 123–128.
[21] J. P. Yu, S. Sun, Y. X. Jiang, X. Y. Ma, F. Chen, G. Y. Zhang, X. H. Fang, *Polymer* **2006**, 47, 2533–2538.
[22] E. Evans, K. Ritchie, *Biophys. J.* **1997**, *72*, 1541–1555.
[23] T. Strunz, K. Oroszlan, I. Schumakovitch, H. J. Güntherodt, M. Hegner, *Biophys. J.* **2000**, *79*, 1206–1212.
[24] M. Guthold, R. Superfine, R. M. Taylor, *Biomed. Microdevices* **2001**, *3*, 9–18.
[25] V. Barsegov, D. Thirumalai, *Proc. Natl. Acad. Sci. USA* **2005**, *102*, 1835–1839.
[26] G. Bell, *Science* **1978**, *200*, 618–627.
[27] L. C. Bock, L. C. Griffin, J. A. Latham, E. H. Vermaas, J. J. Toole, *Nature* **1992**, *355*, 564–566.
[28] J. L. Hutter, J. Bechhoefer, *Rev. Sci. Instrum.* **1993**, *64*, 1868–1873.
[29] I. Schumakovitch, W. Grange, T. Strunz, P. Bertoncini, H. J. Güntherodt, M. Hegner, *Biophys. J.* **2002**, *82*, 517–521.

Received: July 21, 2006
Revised: October 30, 2006

 © 2007 Wiley-VCH Verlag GmbH & Co. KGaA, Weinheim